

Long-term (10^5) or short-term (10^3) $\delta^{13}\text{C}$ excursion near the Palaeocene–Eocene transition: evidence from the Tethys

Gangyi Lu¹, Gerta Keller¹, Thierry Adatte², Nieves Ortiz¹, Eustoquio Molina³

¹Department of Geological & Geophysical Sciences, Princeton University, Princeton, NJ 08544, USA, ²Institut de Géologie, 11 rue Emile Argand, 2007 Neuchâtel, Switzerland, ³Departamento de Geología (Palaeontología), Universidad de Zaragoza, E-50009 Zaragoza, Spain

ABSTRACT

Expanded sedimentary records from the Tethys reveal unique faunal and isotopic changes across the Palaeocene–Eocene (P–E) transition. Unlike in the open oceans, the Tethys exhibits a gradual decrease of 1.5‰ in $\delta^{13}\text{C}$ values prior to the rapid $\delta^{13}\text{C}$ excursion. Associated with the $\delta^{13}\text{C}$ excursion is a decrease in calcite burial, increase in detrital content and appearance of a unique opportunistic planktic foraminiferal assemblage (e.g. compressed acarininids). The existence of a prelude decrease in $\delta^{13}\text{C}$ values in the Tethys suggests that the P–E $\delta^{13}\text{C}$ excursion may have occurred in two steps and over a few hundred thousand years, rather than as one step over a few thousand years as previously suggested. This slower excursion rate is readily explained by changing organic carbon weathering or burial rates and avoids the need of invoking *ad hoc* scenarios.

Terra Nova, 8, 347–355, 1996.

INTRODUCTION

A remarkable short-term global change occurred 54.8 Ma (geomagnetic polarity time-scale of Cande and Kent, 1992) near the Palaeocene–Eocene (P–E) transition. Preliminary studies suggest that this global change took place within a few thousand years (kyr) and lasted less than 200 kyr (Kennett and Stott, 1991). It was characterized by a 6–8 °C warming in the deep ocean and high-latitude surface ocean as indicated by foraminiferal $\delta^{18}\text{O}$ analyses and a major change in the carbon budget as indicated by a negative excursion of 2.5–3‰ (global average) in carbonate $\delta^{13}\text{C}$ values (Kennett and Stott, 1991; Pak and Miller, 1992; Stott, 1992; Koch *et al.*, 1992; Lu and Keller, 1993; Canudo *et al.*, 1995; Bralower *et al.*, 1995; Thomas and Shackleton, 1996; Stott *et al.*, 1996). Associated with these dramatic changes in climate and oceanography, the global ecosystem underwent a sig-

nificant reorganization marked by extinctions in benthic foraminifera, speciation in land mammals, and proliferation of thermophilic species in planktic foraminifera and terrestrial plants (Gingerich, 1986; Thomas, 1990; Wing *et al.*, 1991; Lu and Keller, 1993). Clay mineral compositions suggest a time of exceptionally high precipitation in Antarctica (Robert and Kennett, 1994), but an arid climate in the Tethys region (Adatte *et al.* in prep.), and eolian dust grain size changes suggest a reduction in surface wind intensity which might be related to changes in large-scale atmospheric circulation (Miller *et al.*, 1987; Rea *et al.*, 1990; Hovan and Rea, 1992). Coincident with the $\delta^{13}\text{C}$ excursion, carbonate sedimentation decreased drastically across all major ocean basins as well as on continental margins (O'Connell, 1990; Lu and Keller, 1993; Canudo *et al.*, 1995; Thomas and Shackleton, 1996), indicating significant changes in ocean

chemistry which might have affected atmospheric CO_2 concentrations.

In terms of rate and magnitude, the thermal and geochemical changes across the P–E transition are unprecedented in the geological record. Sea surface temperatures near Antarctica may have reached 20 °C (Kennett and Stott, 1991), the highest values observed over the last 100 million years. Moreover, the timing and amplitude of the $\delta^{13}\text{C}$ excursion suggests that as much as 5 billion tonnes of organic carbon was added into active reservoirs (biosphere, atmosphere and ocean) per year, a rate comparable to anthropogenic fossil fuel burning today (Kennett and Stott, 1991; Zachos *et al.*, 1993; Thomas and Shackleton, 1996). Several hypotheses ranging from enhanced hydrothermal activity on the sea floor to the sudden emission of greenhouse gases have been proposed as potential causal agents of this unusual global change (Owen and Rea, 1985; Rea *et al.*, 1990; Kennett and Stott, 1990, 1991; Sloan *et al.*, 1992; Lu and Keller, 1993; Eldholm and Thomas, 1993; Zachos *et al.*, 1993; Thomas and Shackleton, 1996).

The Tethys is one of the critical regions for investigating the potential cause(s) and mechanism(s) of the P–E global change (Kennett and Stott, 1990, 1991). During the P–E transition, the Tethys was a semi-restricted basin surrounded by vast areas of shallow epicontinental seas (Oberhänsli and Hsü, 1986; Oberhänsli, 1992). This unique geographical feature suggests that the Tethys region was potentially a major source of warm saline deep water (WSDW, Kennett and Stott, 1990, 1991), a possible driving force for the P–E deep ocean warming.

Our current database on the P–E global change is largely based on deep-sea sections. Although these deep-sea sections have yielded P–E sequences with

excellent foraminiferal preservation and high-quality stable isotope data, the critical clay interval in which the $\delta^{13}\text{C}$ excursion occurred is invariably condensed, ranging from centimetres to a few decimetres. As a result, the nature and tempo of the events is often obscured. Recent investigation of the P-E sections from continental margins of the Tethys (Spain, Tunisia, Israel and Egypt) reveals stratigraphically continuous sequences with sediment accumulation rates several times higher than in the deep-sea, and the critical clay layer reaching 1 to several metres in thickness (Molina *et al.*, 1994; Ortiz, 1994; Speijer, 1994; Canudo *et al.*, 1995; Arenillas and Molina, in press). These expanded sections provide the opportunity for building a high-resolution time-scale and examining in detail the regional climatic, oceanographic and biotic changes across the P-E transition. Herein are reported the results of foraminiferal, stable isotopic and whole rock composition analyses from a newly discovered P-E section at Alamedilla in southern Spain, which appears to be formed in a lower bathyal environment. By conducting high-resolution faunal, isotopic and mineralogic analyses, it was possible to document the characteristics of the P-E events in the deep Tethys basin, correlate these events with the deep-sea records, and reveal the detailed pattern for the onset of the isotopic excursion.

MATERIALS AND METHODS

The Alamedilla section is located near the village of Alamedilla, in the Province of Granada, Spain, and is geologically in the Sub-betic Zone (Betic Cordillera). It was sampled at 35 cm intervals between biozones P5x and P7 spanning a total of 30 m and 2.5 Myr. Closely spaced samples at 5 cm intervals were examined across the critical interval of global change (13–15 m) in order to determine the sequential occurrence of the benthic foraminiferal extinction, planktic foraminiferal turnover and details of the $\delta^{13}\text{C}$ excursion. For foraminiferal and stable isotopic analyses, sediments were soaked in water and washed through a 63 μm sieve. Stratigraphic ranges and relative abundances of planktic foraminiferal species for each sample were determined from

counts of a random split of about 300 specimens in the > 106 μm size fraction. The planktic foraminiferal zonation in this study is based on a revision of the P-zonation of Berggren and Miller (1988) by Lu and Keller (1995). Benthic foraminifera were examined in the > 63 μm size fraction to determine the position of the mass extinction. Oxygen and carbon stable isotope analyses were based on monospecific samples, each containing 30 individuals of *Morozovella subbotinae*, a surface-dwelling planktic foraminiferal species. In the eight samples below the first stratigraphic appearance of *M. subbotinae*, a different species, *M. aequa*, which is similar to *M. subbotinae* in morphology and habitat (Lu and Keller, 1996), was analysed. Analyses were conducted at the stable isotope geochemistry laboratory at Princeton University using a VG Optima gas source mass spectrometer equipped with a common acid bath. The results were calibrated to the PDB scale with the standard errors of 0.05‰ for $\delta^{13}\text{C}$ and 0.1‰ for $\delta^{18}\text{O}$. Bulk rock compositional analyses were conducted at the University of Neuchâtel, Switzerland, using a SCINTAG XRD 2000 Diffractometer.

RESULTS

Faunal changes

Figure 1 shows a major faunal turnover in planktic foraminifera between 13.60 and 15.00 m as indicated by the drastic increases in relative species turnover rates and the relative abundance of compressed acarininids. The relative species turnover rate is based on the percentage of first and last appearances normalized to sample the resolution, and can be calculated by:

$$\frac{\text{First and last appearances} \times 100}{(\text{Species richness}) \times (\text{sample spacing}) / (\text{mean sample spacing})}$$

The background turnover rates throughout the entire interval are less than 5%. During the P-E turnover, relative turnover rates increased to as high as 33%. The twin peaks in the species turnover rates coincide with the onset and end of the turnover event (Fig. 1). A pre-P-E faunal change with smaller magnitude (18%) is recorded near the P5x/P6a

biozone boundary. The compressed acarininids are composed of three acarininid species (e.g. *A. africana*, *A. sabaiyaensis* and *A. berggreni*) that were first described by El-Naggar (1966) from the Esna-Ildfu region of Egypt near the P-E transition. At Alamedilla, their ranges are confined within the P-E faunal turnover interval where they reached a maximum combined relative abundance of 33% (Fig. 1). Similar species have recently been reported from the equatorial Pacific Site 865 within the isotopic excursion interval (Kelly *et al.*, 1995).

Benthic foraminiferal data indicate that deposition across the P-E transition at Alamedilla occurred in a lower bathyal to abyssal environment. The fauna contains abundant (up to 27%) abyssaminids and many species that have their upper depth limits between 1000 and 2000 m (e.g. *Abyssamina poagi*, *Bulimina velascoensis*, *Aragonia aragonensis* and *Tritaxia palaeoecnica*). The benthic foraminiferal mass extinction was located at 13.45 m (Fig. 1) as marked by the disappearance of *Stensioina beccariiiformis*, among other species. About 53% of the late Palaeocene species survived into the lower Eocene.

Stable isotope changes

Stable isotope measurements were conducted on *Morozovella subbotinae*, a surface-dwelling planktic foraminiferal species. The results demonstrate little change in $\delta^{18}\text{O}$ values across the P-E transition, but a distinct negative excursion in $\delta^{13}\text{C}$ values that peaks in the interval of maximum planktic foraminiferal turnover (Fig. 1). Comparison with the results from other Tethys sections and low-latitude deep-sea sites indicates that the planktic $\delta^{18}\text{O}$ and $\delta^{13}\text{C}$ patterns observed at Alamedilla represent true signals. Foraminiferal isotope analyses from tropical-subtropical Pacific Sites 47.2, 577 and 865 show no significant changes in planktic $\delta^{18}\text{O}$ values, but a negative excursion in benthic $\delta^{18}\text{O}$ values; negative $\delta^{13}\text{C}$ excursions are present in both planktic and benthic foraminifera (Stott, 1992; Pak and Miller, 1992; Bralower *et al.*, 1995). In the Tethys region, benthic isotope analyses were conducted at Caravaca, Spain, by Canudo *et al.* (1995) which show excursions in both $\delta^{18}\text{O}$ and $\delta^{13}\text{C}$ values. Thus, the planktic and benthic isotopic patterns

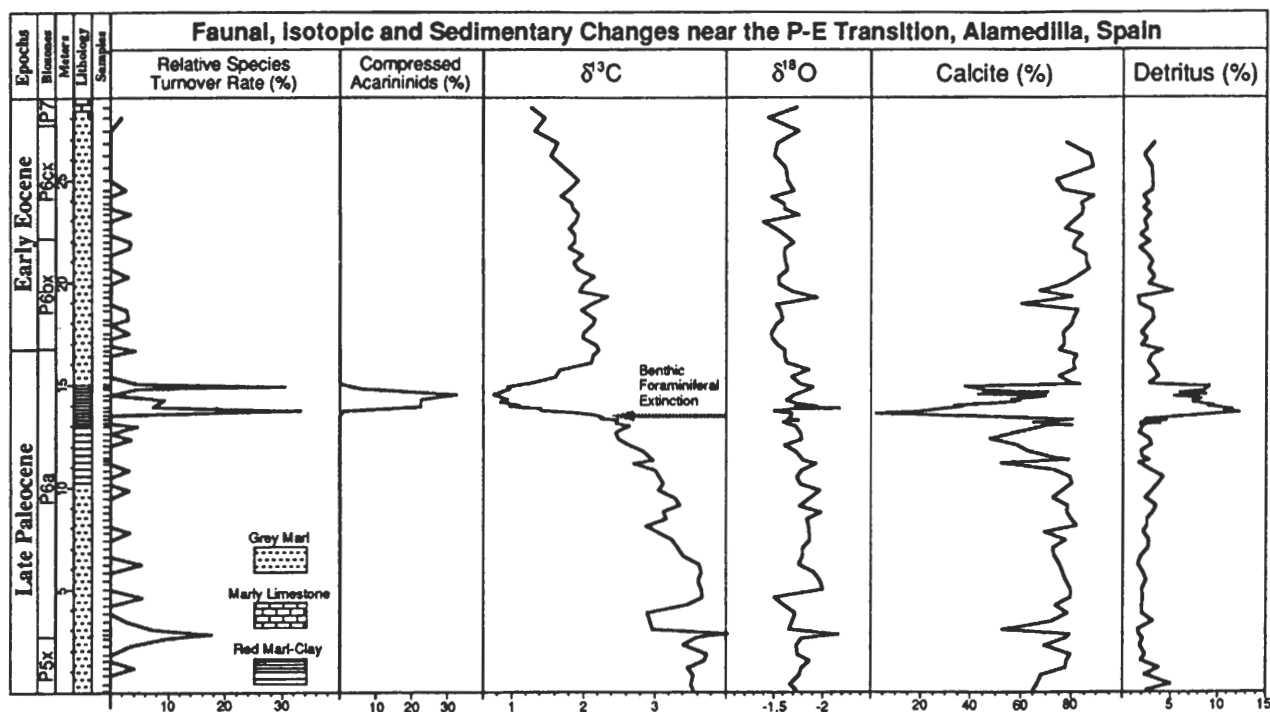


Fig. 1. Foraminiferal faunal, isotopic and sediment compositional changes across the Palaeocene–Eocene transition at Alamedilla, Spain. The relative species turnover rate is based on the percentage of first and last appearances normalized to the sample resolution. Compressed acarininids include species *A. africana*, *A. sabaiyaensis* and *A. berggreni*. Stable isotope values are calibrated to PDB standard with the standard errors of 0.05‰ for $\delta^{13}\text{C}$ and 0.1 for $\delta^{18}\text{O}$. Note the correlation between the planktic foraminiferal turnover, benthic foraminiferal extinction, $\delta^{13}\text{C}$ excursion, decrease in calcite content and increase in detrital content near the P–E transition.

observed in the Tethys region are consistent with those observed from other low-latitude deep-sea sequences.

The $\delta^{13}\text{C}$ excursion at Alamedilla can be divided into several stages indicating the progressive $\delta^{13}\text{C}$ changes across the P–E transition (Fig. 1). Between 0 m and 6.40 m, planktic $\delta^{13}\text{C}$ values are relatively stable at 3.5‰. In the middle of this interval, $\delta^{13}\text{C}$ values fluctuate near the P5x/P6a biozone boundary, coincident with the pre-P–E faunal change. From 6.40 m to 13.25 m, planktic $\delta^{13}\text{C}$ values gradually decrease by 1‰. Following this gradual decrease is the interval of the P–E $\delta^{13}\text{C}$ excursion between 13.25 m and 16.05 m. The onset of this excursion is recorded in a 0.70 m interval between 13.25 m and 13.95 m as marked by a rapid decrease of 1.7‰. Between 13.95 m and 14.90 m, planktic $\delta^{13}\text{C}$ values remain at the lowest level (< 1‰) of the entire observed interval. A gradual recovery begins at 15.05 m and ends at 16.05 m. Above 16.05 m, planktic $\delta^{13}\text{C}$ values decrease gradually, forming part of the long term decrease in oceanic $\delta^{13}\text{C}$

values that characterizes the late Palaeocene to the early Eocene (Shackleton, 1986, 1987). The beginning of the rapid excursion in planktic $\delta^{13}\text{C}$ values occurred 0.20 m below the benthic foraminiferal extinction and 0.35 m below the onset of the planktic foraminiferal turnover. The pre-excursion gradual decrease in $\delta^{13}\text{C}$ values began well below these faunal changes and has not been observed at other continental margin or deep-sea sites outside the Tethys region.

Whole rock composition

Sediments of the Alamedilla section are composed of calcite, phyllosilicates and detritus. Whole-rock compositional analyses show that calcite content averages 75–80% over the lower 10 m of the section (Fig. 1). A gradual but fluctuating decrease in calcite content starts at 10.30 m and accelerates at 13.45 m. Coincident with the $\delta^{13}\text{C}$ excursion and planktic foraminiferal turnover, calcite content drops to as low as 2% and averages 44% between 13.45 m and

15.00 m. At 15.00 m, calcite content rapidly returns to 75–85% and remains high through the upper portion of the section. Detrital content, measuring the relative abundance of detrital quartz, K-feldspar and plagioclase, averages 2–4% through most of the section except for the $\delta^{13}\text{C}$ excursion interval between 13.45 m and 15.00 m (Fig. 1). Within this interval detrital content increases to a high of 12% and averages 9%. Changes in calcite and detrital contents are compensated by changes in phyllosilicate contents. These changes in sedimentary composition and their association with the $\delta^{13}\text{C}$ excursion, benthic foraminiferal extinction and planktic foraminiferal turnover are similar to the patterns observed at Caravaca across the P–E transition (Canudo *et al.*, 1995; Adatte *et al.*, in prep.).

DISCUSSION

Chronostratigraphy

A high-resolution chronostratigraphy is crucial when evaluating P–E changes

which took place over a few thousand years (Kennett and Stott, 1991). Since Chron 24r lasts more than 3 million years across the P-E transition (Berggren *et al.*, 1985; Cande and Kent, 1992), possible changes in sedimentation rates during C24r need to be examined by biostratigraphy and chemostratigraphy. For the Alamedilla section, age models can be developed independently through foraminiferal biostratigraphy and $\delta^{13}\text{C}$ stratigraphy. An age model based on faunal changes and planktic foraminiferal datum events is shown in Fig. 2 with model parameters listed in Table 1. All ages in this model are calibrated to the geomagnetic polarity time-scale (GPTS) of Cande and Kent (1992) based on the discussion by Lu and Keller (1995). Calibration with the GPTS by Berggren *et al.* (1985) is also shown in Table 1. This age model indicates relatively uniform sedimentation rates of 2.4 cm kyr^{-1} for the lower part of the section from the base up to 15.00 m. Above 15.00 m, sedimentation rates drop significantly to 0.7 cm kyr^{-1} . This change in sedimentation rates coincides with a major lithological transition as marked by the sudden increase in calcite content from an average of 44% between 13.45 m and 15.00 m to an average of 78% above 15.00 m (Fig. 1). The main phase of the P-E event is recorded in a 1.55 m interval between 13.45 m and 15.00 m. The $\delta^{13}\text{C}$ excursion, however, is recorded over a much more expanded interval between 13.25 m and 16.05 m. This expanded record of the red, clay-rich layer at Alamedilla is also documented by the sequential occurrence of the benthic foraminiferal extinction and the $\delta^{13}\text{C}$

excursion which in the deep-sea and other continental margin sites appear to occur simultaneously (Kennett and Stott, 1991; Pak and Miller, 1992; Stott, 1992; Lu and Keller, 1993; Canudo *et al.*, 1995; Thomas and Shackleton, 1996; Bralower *et al.* 1995). We use the age model in Fig. 2 to calibrate $\delta^{13}\text{C}$ values from Alamedilla to the age scale (Fig. 3). Foraminiferal $\delta^{13}\text{C}$ values from ODP Site 690 (one of the most complete deep-sea section for this interval, Kennett and Stott, 1991) are calibrated to the age scale based on magnetostratigraphy (Spiess, 1990). Correlation with the equatorial Pacific Site 865 is based on $\delta^{13}\text{C}$ stratigraphy. Comparison of $\delta^{13}\text{C}$ excursion patterns between these sections allows us to examine the consistency between foraminiferal and $\delta^{13}\text{C}$ stratigraphies (Fig. 3).

This integrated biostratigraphic and chemostratigraphic approach reveals both the validity and potential problems of the age model for the Alamedilla section. Above the rapid $\delta^{13}\text{C}$ shift (13.25 m), foraminiferal and $\delta^{13}\text{C}$ chronostratigraphies are consis-

tent as indicated by the full range correlation of the $\delta^{13}\text{C}$ excursion at Alamedilla with Sites 690 and 865 (Fig. 3). Below the $\delta^{13}\text{C}$ shift, however, inconsistency between foraminiferal and $\delta^{13}\text{C}$ chronostratigraphies is shown by a prelude decrease in $\delta^{13}\text{C}$ values prior to the rapid excursion at Alamedilla which is not observed at Site 690 or 865 (Fig. 3).

Expanded or unique record

The prelude decrease in $\delta^{13}\text{C}$ values prior to the rapid excursion at Alamedilla posts problems for present

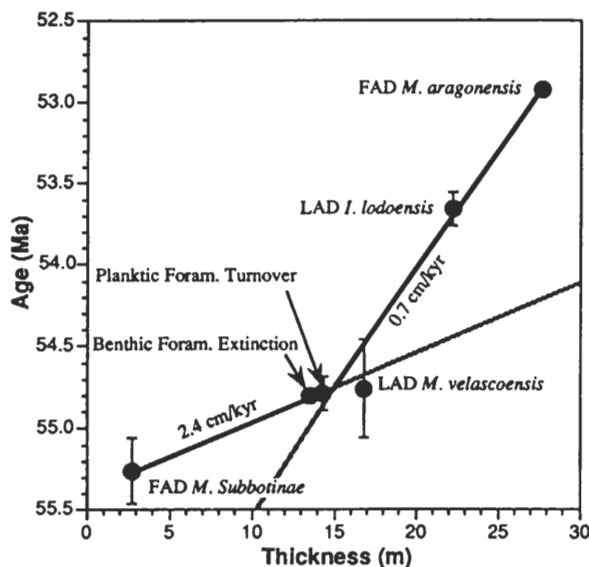


Fig. 2. Age model based on the datum and faunal events of foraminifera as listed in Table 1. Absolute ages are calibrated to the geomagnetic polarity time scale of Cande and Kent (1992) according to the discussion by Lu and Keller (1995). Note the change in sedimentation rates below and above 15 m.

Table 1 Age model parameters for the Alamedilla section.

Events	Calibration to the GPTS (Ma)*			Position (m) at Alamedilla
	Berggren <i>et al.</i> (1985)	Cande and Kent (1992)	Error (\pm)	
FAD <i>M. aragoensis</i>	55.67	52.92	0.00	27.70
LAD <i>I. Iodoensis</i>	56.49	53.64	0.09	22.13
LAD <i>M. velascoensis</i>	57.52	54.75	0.29	16.78
Planktic Foram. Turnover	57.54	54.78	0.10	14.30
Benthic Foram. Extinction	57.56	54.80	0.01	13.45
$\delta^{13}\text{C}$ Excursion	57.56	54.80	0.00	13.25
FAD <i>M. subbotinae</i>	57.98	55.26	0.19	2.70

*Absolute ages and errors are calibrated to the geomagnetic polarity time scales by Berggren *et al.* (1985) and Cande and Kent (1992) based on the discussion by Lu and Keller (1995).

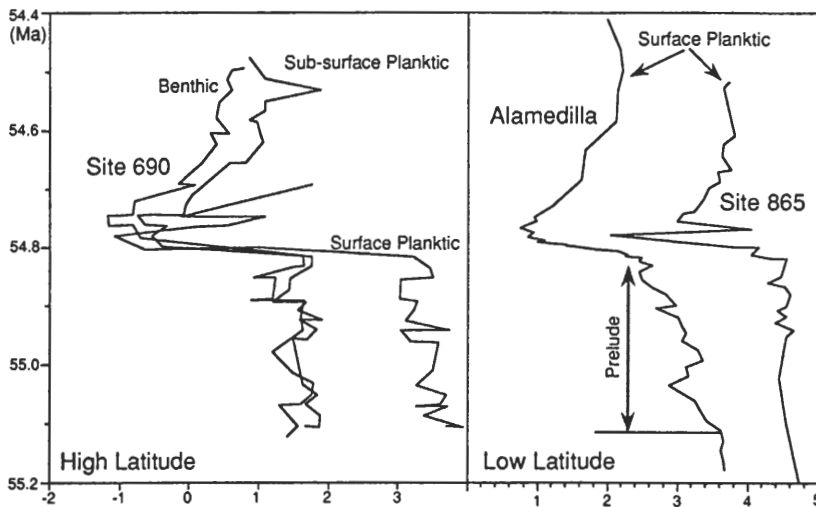


Fig. 3. Correlation of the foraminiferal $\delta^{13}\text{C}$ excursion between Alamedilla and Sites 690 and 865. Isotopic data of the two deep-sea sites are from Kennett and Stott (1991) and Bralower *et al.* (1995). Note the distinct prelude decrease in $\delta^{13}\text{C}$ values prior to the rapid excursion at Alamedilla and the $\delta^{13}\text{C}$ offset between the Alamedilla section and Site 865.

chronostratigraphies across the P–E transition. In the foraminiferal age model used in this study, only one control point (FAD of *M. subbotinae*) is provided below the $\delta^{13}\text{C}$ excursion with an error of ± 190 kyr (Fig. 2). $\delta^{13}\text{C}$ stratigraphy can not be used to correlate the prelude decrease interval because it has not been observed at other sections outside the Tethys region. It is thus impossible to correlate the prelude $\delta^{13}\text{C}$ decrease interval between Alamedilla and deep-sea sites to a precision higher than a few hundred-thousand years. However, foraminiferal and $\delta^{13}\text{C}$ stratigraphies allow us to examine whether this prelude $\delta^{13}\text{C}$ decrease is part of the long-term trend or related to the short-term excursion.

A long-term global decrease in foraminiferal $\delta^{13}\text{C}$ values started in the middle part of the late Palaeocene and lasted through the middle part of the early Eocene (Shackleton, 1986, 1987). The beginning of this long-term decrease is dated 2.5 Myr before the short-term excursion and nearly 2 Myr prior to the FAD of *M. subbotinae* (Shackleton, 1986; Stott *et al.*, 1990; Corfield and Cartlidge, 1992). The prelude decrease in $\delta^{13}\text{C}$ values at Alamedilla occurred after the FAD of *M. subbotinae* and is estimated to have occurred 300 kyr prior to the short-term $\delta^{13}\text{C}$ excursion based on the foraminiferal stratigraphy (Figs 1 and 3). Thus,

there is a 2 Myr difference between the beginning of the long term global $\delta^{13}\text{C}$ decrease and the prelude $\delta^{13}\text{C}$ decrease at Alamedilla. Within the precision of foraminiferal stratigraphy (Berggren *et al.*, 1985; Lu and Keller, 1995), it is concluded here that the prelude decrease at Alamedilla is related to the short-term $\delta^{13}\text{C}$ excursion rather than the long-term $\delta^{13}\text{C}$ decrease.

The presence of this prelude $\delta^{13}\text{C}$ decrease at Alamedilla, in contrast to its apparent absence in deep-sea sites, may be explained by an expanded sedimentary record at Alamedilla. This is suggested by: (i) high sedimentation rates at Alamedilla (2.4 cm kyr^{-1} for the lower part of the section without correction for compaction, Fig. 2); (ii) sequential occurrence of the $\delta^{13}\text{C}$ excursion, benthic foraminiferal extinction, and planktic foraminiferal turnover (Table 1), as compared with their simultaneous occurrences in the deep sea; and (iii) a > 2 m clay-rich layer as compared with the deep sea where this clay layer is only a few centimetres to decimetres thick. In contrast to the Alamedilla section, the deep-sea record may be highly condensed or contain a short hiatus of 300 kyr at the base of the $\delta^{13}\text{C}$ excursion (Aubry *et al.*, 1996). If this is the case, the onset of the short-term $\delta^{13}\text{C}$ excursion might have occurred over a much longer interval than previously estimated.

Alternatively, the presence of a prelude $\delta^{13}\text{C}$ decrease at Alamedilla may be due to unique oceanographic conditions in the Tethys. This is suggested by comparing $\delta^{13}\text{C}$ values between the Alamedilla section and deep-sea sites (Fig. 3). Surface planktic $\delta^{13}\text{C}$ values are measured using the species *Morozovella subbotinae* at the Alamedilla section, *Morozovella velascoensis* at Site 865, and *Acarinina praepentacamerata* at Site 690. Therefore, interspecific $\delta^{13}\text{C}$ variations must be considered when comparing $\delta^{13}\text{C}$ values between these sections. Pairing measurement shows that *M. velascoensis* is heavier than *M. subbotinae* by 0.04‰ in $\delta^{13}\text{C}$ values (Shackleton *et al.*, 1985; Lu and Keller, 1996), an offset smaller than machine errors. In contrast, *M. subbotinae* is heavier than *A. praepentacamerata* by 0.63‰ (Lu and Keller, 1996). If these interspecific offsets are adjusted, Sites 690 and 865 will have similar surface planktic $\delta^{13}\text{C}$ values prior to the excursion, whereas $\delta^{13}\text{C}$ values of the Alamedilla section will be 1–2‰ lighter than those of the two deep-sea sites. Such a major $\delta^{13}\text{C}$ offset between the Alamedilla section and deep-sea sites indicates the uniqueness of the Tethys environment. In this case, both the Alamedilla and deep-sea $\delta^{13}\text{C}$ records may be largely complete and the different patterns in $\delta^{13}\text{C}$ values prior to the global short-term excursion (Fig. 3) reflect true differences in palaeoceanographic conditions between the Tethys and the open oceans.

P–E $\delta^{13}\text{C}$ excursion: two scenarios

The P–E $\delta^{13}\text{C}$ excursion has been observed in all major ocean basins (Kennett and Stott, 1991; Pak and Miller, 1992; Stott, 1992; Lu and Keller, 1993; Canudo *et al.*, 1995; Bralower *et al.*, 1995; Thomas and Shackleton, 1996) as well as on land (Koch *et al.*, 1992; Stott *et al.*, 1996). A typical shape of this excursion in the deep sea is shown in Fig. 3 based on foraminiferal $\delta^{13}\text{C}$ analysis from ODP Site 690, which shows relatively stable pre-excursion values, a rapid negative excursion and a gradual recovery (Kennett and Stott, 1991). The presence of a prelude gradual decrease prior to the rapid excursion at Alamedilla suggests alternative interpretations for this carbon isotope event.

Rapid Excursion Scenario

If both Alamedilla and deep-sea $\delta^{13}\text{C}$ records are largely complete, all previous interpretations about the global P-E $\delta^{13}\text{C}$ excursion remain valid, including: (i) rapid excursion over a few thousand years (Kennett and Stott, 1991; Stott, 1992; Thomas and Shackleton, 1996); and (ii) a magnitude of 2.5–3‰ as global average which may be as large as 4.5–5‰ regionally (Kennett and Stott, 1991; Stott, 1992; Pak and Miller, 1992; Lu and Keller, 1993; Bralower *et al.*, 1995; Thomas and Shackleton, 1996). The total magnitude (including the prelude decrease) of the $\delta^{13}\text{C}$ excursion at Alamedilla is 2.7‰ and hence close to the global average. It differs in that the excursion includes two stages, the prelude and the abrupt shift (Fig. 3). During the prelude stage, $\delta^{13}\text{C}$ values decrease by 1–1.2‰ over a period of as long as 300 kyr. The prelude decrease is accompanied by decreased calcite concentrations in sediments (Fig. 1). Many regional processes can explain this gradual decrease in $\delta^{13}\text{C}$ values and calcite concentration, including decreased surface productivity and increased input of organic matter to the Tethys basin. The prelude decrease is followed by a rapid excursion of 1.5–1.7‰ in $\delta^{13}\text{C}$ values, which is coeval with the global $\delta^{13}\text{C}$ excursion, although at a much reduced magnitude (Fig. 3). This rapid excursion is associated with a mass extinction in benthic foraminifera and a major faunal turnover in planktic foraminifera (Fig. 1) that have been observed at many deep-sea, as well as near-shore sections (see Lu and Keller, 1995; Thomas and Shackleton, 1996 for reviews). The occurrence and high relative abundance of the opportunistic planktic foraminiferal species (e.g. compressed acarininids) at Alamedilla and Site 865 suggests a unique oceanic environment during the isotopic excursion. Associated with the $\delta^{13}\text{C}$ excursion at Alamedilla is an increase in detrital content (Fig. 1), which suggests changes in ocean currents and/or surface winds during the P-E transition.

Slow Excursion Scenario

The negative $\delta^{13}\text{C}$ excursion was estimated to have occurred over a few thousand years based on deep-sea re-

ords (Kennett and Stott, 1991; Stott, 1992; Pak and Miller, 1992; Lu and Keller, 1993; Thomas and Shackleton, 1996). However, if the discrepancy between the $\delta^{13}\text{C}$ records from Alamedilla and deep sea is the result of differences in sedimentation rates, the timing of the $\delta^{13}\text{C}$ excursion may have been underestimated significantly. Foraminiferal biostratigraphy at Alamedilla suggests that the $\delta^{13}\text{C}$ excursion occurred gradually over 300 kyr (Fig. 3). Although this estimate has an error margin of ± 124 kyr (based on the error in the FAD of *M. subbotina*; Table 1), it represents a significantly longer interval. A slow $\delta^{13}\text{C}$ excursion over a few hundred thousand years is readily explained by changing organic carbon weathering or burial rates (Bernier, 1992; Raymo and Ruddiman, 1992; Selverstone and Gutzler, 1993). In contrast, a rapid $\delta^{13}\text{C}$ excursion of 2–3‰ over a few thousand years implies a fast release of isotopically light carbon from huge carbon reservoirs that remain an enigma (Kennett and Stott, 1991; Stott, 1992; Zachos *et al.*, 1993; Thomas and Shackleton, 1996).

CONCLUSION

Expanded sedimentary records from Alamedilla, Spain, reveal unique faunal, isotopic and sediment compositional changes across the Palaeocene–Eocene (P–E) transition. Unlike in the open oceans, the Alamedilla section exhibits a gradual decrease of 1‰ in $\delta^{13}\text{C}$ values prior to the rapid $\delta^{13}\text{C}$ excursion. Associated with the $\delta^{13}\text{C}$ excursion is a decrease in calcite preservation, increase in detrital content and appearance of some unique planktic foraminiferal species (e.g. compressed acarininids). Foraminiferal and $\delta^{13}\text{C}$ stratigraphies suggest that the prelude $\delta^{13}\text{C}$ decrease is related to the short-term $\delta^{13}\text{C}$ event rather than the long-term trend. The existence of this prelude decrease suggests that the rapid $\delta^{13}\text{C}$ excursion, currently estimated to have occurred over a few thousand years based on deep-sea records, may have occurred at a much slower rate over a few hundred thousand years. This significantly slower excursion rate can be easily explained by changing organic carbon weathering and/or burial rates and, thus, avoids the need for *ad hoc* scenarios.

ACKNOWLEDGEMENTS

We thank D. Schrag for many discussions and for conducting stable isotope measurements in the stable isotope geochemistry laboratory of Princeton University. P. Koch and W. Wei provided important comments and suggestions on an early draft. This study was supported by NSF grant OCE-9021338, Swiss National Fund no. 8220–028367 and post-doctoral fellowship EX92–1721 5112 from the Spanish Ministry of Education and Science.

REFERENCES

- Arenillas I. and Molina E. (in press) Biostratigrafía y evolución de las asociaciones de foraminíferos planctónicos del tránsito Paleoceno–Eoceno en Alamedilla (Cordilleras Béticas), *Rev. Esp. Micropaleont.*
- Aubry, M.-P., Berggren W. A., Stott L. D. and Sinha A. (1996) The upper Paleocene–lower Eocene stratigraphic record and the Paleocene/Eocene boundary carbon isotope excursion, *Spec. Publ. Geol. Soc. London.*, **101**, 353–380.
- Berggren W. A., Kent D. V. and Flynn J. J. (1985) Paleogene geochronology and chronostratigraphy. In: *Geochronology and the Geological Record* (ed. by N. J. Snelting). *Mem. Geol. Soc. London*, **10**, 211–260.
- Berggren W. A. and Miller K. G. (1988) Paleogene planktic foraminiferal biostratigraphy and magnetobiostratigraphy, *Micropaleontology*, **34**, 362–380.
- Berner R. A. (1992) A model for atmospheric CO_2 over Phanerozoic time, *Am. J. Sci.*, **291**, 339–376.
- Bralower T. J., Zachos J. C., Thomas E., Parrow M., Paul C. K., Kelly D. C., Premoli Silva I., Sliter W. V. and Lohmann K. C. (1995) Late Paleocene to Eocene paleoceanography of the equatorial Pacific Ocean: Stable isotopes recorded at Ocean Drilling Program Site 865, Allison Guyot, *Paleoceanography*, **10**, 841–865.
- Brass G. W., Southam J. R. and Peterson W. H. (1982) Warm saline bottom water in the ancient ocean, *Nature*, **296**, 620–623.
- Cande S. C. and Kent D. V. (1992) A new geomagnetic polarity time scale for the Late Cretaceous and Cenozoic, *J. geophys. Res.*, **97**, 13917–13951.
- Canudo J. I., Keller G., Molina E. and Ortiz N. (1995) Planktic foraminiferal turnover and $\delta^{13}\text{C}$ isotopes across the Paleocene–Eocene transition at Caravaca and Zumaya, Spain, *Palaeogeogr. Palaeoclim. Palaeoecol.*, **114**, 75–100.

- Corfield R. M. and Cartlidge J. E. (1992) Oceanographic and climatic implications of the Palaeocene carbon isotope maximum, *Terra Nova*, **4**, 443–455.
- El-Naggar Z. R. (1966) Stratigraphy and planktonic foraminifera of the Upper Cretaceous-Lower Tertiary succession in the Esna-Idfu region, Nile Valley, Egypt. In: *U.A.R. British Mus. (Nat. Hist.), Bull.*, London, Geol. Suppl., no. 2.
- Eldholm O. and Thomas E. (1993) Environmental impact of volcanic margin formation, *Earth Planet. Sci. Lett.*, **117**, 319–329.
- Gingerich P. D. (1986) Evolution and the fossil record: patterns, rates, and processes, *Can. J. Zool.*, **65**, 1053–1060.
- Hoven S. A. and Rea D. K. (1992) Paleocene/Eocene boundary changes in atmospheric and oceanic circulation: A Southern Hemisphere record, *Geology*, **20**, 15–18.
- Kelly D. C., Bralower T. J., Zachos J. C., Thomas E. and Premoli Silva I. (1995) Rapid diversification of tropical Pacific planktonic foraminifera during the late Paleocene thermal maximum, *Abstract with Programs*, GSA.
- Kennett J. P. and Stott L. D. (1990) Proteus and Proto-Oceanus: Paleogene oceans as revealed from Antarctic stable isotopic results, *Proc. ODP, Sci. Results*, **113**, 865–879.
- Kennett J. P. and Stott L. D. (1991) Abrupt deep-sea warming, palaeoceanographic changes and benthic extinctions at the end of the Palaeocene, *Nature*, **353**, 225–229.
- Koch P. L., Zachos J. C. and Gingerich P. D. (1992) Correlation between isotope records in marine and continental carbon reservoirs near the Palaeocene/Eocene boundary, *Nature*, **358**, 319–322.
- Lu G. and Keller G. (1993) The Paleocene-Eocene transition in the Antarctic Indian Ocean: Inference from planktic foraminifera, *Mar. Micropaleont.*, **21**, 101–142.
- Lu G. and Keller G. (1995) Planktic foraminiferal faunal turnovers in the subtropical Pacific during the late Paleocene to early Eocene, *J. Foram. Res.*, **25**, 97–116.
- Lu G. and Keller G. (1996) Separating ecological assemblages using stable isotope signals: late Paleocene to early Eocene planktic foraminifera, DSDP Site 577, *J. Foram. Res.*, **26**, 103–112.
- Miller K. G., Janecek T. R., Katz M. E. and Keil D. J. (1987) Abyssal circulation and benthic foraminiferal changes near the Paleocene/Eocene boundary, *Paleoceanography*, **2**, 741–761.
- Molina E., Canudo J. I., Martinez-Ruiz F. and Ortiz N. (1994) Integrated stratigraphy across the Paleocene/Eocene boundary at Caravaca, southern Spain, *Eclog. geol. Helv.*, **87**, 47–61.
- Oberhänsli H. (1992) The influence of the Tethys on the bottom waters of the early Tertiary ocean. In: *The Antarctic Paleoenvironment: A Perspective on Global Change* (ed. by J. P. Kennett). *Antarctic Research Series*, **56**, 167–184.
- Oberhänsli H. and Hsü K. J. (1986) Paleocene-Eocene paleoceanography. In: *Mesozoic and Cenozoic Oceans*, Geodynamics Series, **15**, 85–100.
- O'Connell S. B. O. (1990) Variations in upper Cretaceous and Cenozoic calcium carbonate percentages, Maud Rise, Weddell Sea, Antarctica, *Proc. ODP, Sci. Results*, **113**, 971–984.
- Ortiz N. (1994) Mass extinction of benthic foraminifera at the Paleocene/Eocene boundary. In: *Extinction and the Fossil Record* (ed. by E. Molina). Cuadernos interdisciplinarios, Seminario Interdisciplinar Universidad Zaragoza, **5**, 201–218.
- Owen R. M. and Rea D. K. (1985) Sea floor hydrothermal activity links climate to tectonics: The Eocene CO₂ greenhouse, *Science*, **227**, 166–169.
- Pak D. K. and Miller K. G. (1992) Paleocene to Eocene benthic foraminiferal isotopes and assemblages: implications for deep-water circulation, *Paleoceanography*, **7**, 405–422.
- Raymo M. E. and Ruddiman W. F. (1992) Tectonic forcing of late Cenozoic climate, *Nature*, **359**, 117–122.
- Rea D. K., Zachos J. C., Owen R. M. and Gingerich P. D. (1990) Global changes at the Paleocene-Eocene boundary: climate and evolutionary consequences of tectonic events, *Palaeogeogr. Palaeoclim. Palaeoecol.*, **79**, 117–128.
- Robert C. and Kennett J. P. (1994) Antarctic subtropical humid episode at the Paleocene-Eocene boundary: Clay-mineral evidence, *Geology*, **22**, 211–214.
- Silverstone J. and Gutzler D. S. (1993) Post-125 Ma carbon storage associated with continent-continent collision, *Geology*, **21**, 885–888.
- Shackleton N. J. (1986) Paleogene stable isotope events, *Palaeogeogr. Palaeoclim. Palaeoecol.*, **57**, 91–102.
- Shackleton N. J. (1987) The carbon isotope record of the Cenozoic: History of organic carbon burial and of oxygen in the ocean and atmosphere. In: *Marine Petroleum Source Rocks* (ed. by J. Brooks and A. J. Fleet). *Spec. Publ. Geol. Soc. London*, **26**, 423–434.
- Shackleton N. J., Corfield R. M. and Hall M. A. (1985) Stable isotope data and ontogeny of Paleocene planktic Foraminifera, *J. Foram. Res.*, **15**, 321–336.
- Sloan L. C., Walker J. C. G., Moore, T. C. Jr. Rea D. K. and Zachos J. C. (1992) Possible methane-induced polar warming in the early Eocene, *Nature*, **357**, 320–322.
- Speijer R. P. (1994) Extinction and recovery patterns in benthic foraminiferal paleo-communities across the Cretaceous/Paleogene and Paleocene/Eocene boundaries, PhD thesis, Universiteit Utrecht, *Geol. Ultraieet.*, No.124., 191p.
- Spieg V. (1990) Cenozoic magnetostratigraphy of Leg 113 drill sites, Maud Rise, Weddell Sea, Antarctica, *Proc. ODP. Sci. Results*, **113**, 261–315.
- Stott L. D. (1992) Higher temperatures and lower oceanic PCO₂: a climate enigma at the end of the Paleocene Epoch, *Paleoceanography*, **7**, 395–404.
- Stott L. D., Kennett J. P., Shackleton N. J. and Corfield R. M. (1990) The evolution of Antarctic surface waters during the Paleogene: Inferences from the stable isotopic composition of planktonic foraminifera, ODP Leg 113, *Proc. ODP, Sci. Results*, **113**, 849–863.
- Stott L. D., Sinha A., Tiry M., Aubry M.P. and Berggren W. A. (1996) The transfer of ¹²C changes from the ocean to the terrestrial biosphere across the Paleocene/Eocene boundary: criteria for terrestrial-marine correlations, *Spec. Publ. Geol. Soc. London.*, **101**, 381–400.
- Thomas E. (1990) Late Cretaceous through Neogene deep-sea benthic foraminifera (Maud Rise, Weddell Sea, Antarctica), *Proc. ODP, Sci. Results*, **113**, 571–594.
- Thomas E. and Shackleton N. J. (1996) The latest Palaeocene benthic foraminiferal extinction and stable isotope anomalies. *Spec. Publ. Geol. Soc. London*, **101**, 401–441.
- Wing S. L., Bown T. M. and Obradovich J. D. (1991) Early Eocene biotic and climatic change in interior western America, *Geology*, **19**, 1189–1192.
- Zachos J. C., Lohmann K. C., Walker J. C. G. and Wise S. W. (1993) Abrupt climate change and transient climates during the Paleogene: a marine perspective, *J. Geol.*, **101**, 191–213.
- Zachos J. C., Stott L. D. and Lohmann K. C. (1994) Evolution of early Cenozoic temperatures, *Paleoceanography*, **9**, 353–387.

Received 10 May 1995; revision accepted 27 February 1996.

Appendix. Data table for Figure 1.

Sample	cm	Age (Myr)	$\delta^{13}\text{C}$	$\delta^{18}\text{O}$	Turnover Rate (%)	(%) Comp. Acarininids	Calcite	Detritus
ala-10	10	55.37	3.54	-1.73	0.0	0.0	64.72	2.49
ala-35	35	55.36	3.52	-1.67	0.0	0.0	66.46	5.00
ala-80	80	55.34	3.54	-1.76	0.0	0.0	67.96	2.38
ala-115	115	55.32	3.46	-1.78	4.1	0.0	77.61	3.75
ala-150	150	55.31	3.71	-1.87	0.0	0.0	77.76	1.91
ala-180	180	55.30	3.73	-1.74	0.0	0.0	79.42	2.37
ala-225	225	55.28	3.41	-1.73	3.6	0.0	69.27	1.79
ala-260	260	55.26	3.59	-1.78	9.5	0.0	77.34	2.15
ala-280	280	55.25	4.03	-2.16	17.6	0.0	79.05	1.72
ala-300	300	55.25	2.98	-1.66	7.3	0.0	52.88	1.57
ala-340	340	55.23			2.8	0.0	71.88	3.16
ala-380	380	55.21	2.89	-1.72	0.0	0.0	78.28	2.07
ala-420	420	55.20	3.47	-1.61	0.0	0.0	73.51	2.00
ala-460	460	55.18	3.67	-1.50	5.5	0.0	79.58	2.10
ala-500	500	55.16	3.65	-2.00	0.0	0.0	79.68	2.00
ala-540	540	55.15	3.61	-1.97	0.0	0.0	77.61	2.48
ala-580	580	55.13	3.65	-1.91	0.0	0.0	76.47	2.16
ala-620	620	55.11	3.62	-1.75	5.3	0.0	75.06	1.59
ala-660	660	55.10	3.41	-1.80	0.0	0.0	73.21	1.94
ala-700	700	55.08	3.32	-1.80	0.0	0.0	72.35	2.62
ala-740	740	55.06	3.25	-1.87	0.0	0.0	77.47	2.79
ala-780	780	55.05			3.3	0.0	69.17	2.08
ala-805	805	55.04	2.88	-1.86	0.0	0.0	81.80	2.59
ala-840	840	55.02	3.16	-1.84	0.0	0.0	79.37	2.49
ala-875	875	55.01	3.11	-1.98	0.0	0.0	77.96	3.18
ala-905	905	54.99	3.35	-1.76	0.0	0.0	78.42	3.46
ala-945	945	54.98	3.29	-1.87	0.0	0.0	72.23	2.38
ala-985	985	54.96	3.06	-1.97	3.1	0.0		
ala-1015	1015	54.95	3.12	-1.77	0.0	0.0	79.92	3.66
ala-1045	1045	54.94	3.07	-1.73	0.0	0.0	78.93	4.24
ala-1080	1080	54.92	3.00	-1.79	3.1	0.0	72.81	2.86
ala-1115	1115	54.91	2.70	-1.93	0.0	0.0	52.25	1.73
ala-1130	1130	54.90	2.97	-1.81	0.0	0.0	78.53	2.77
ala-1145	1145	54.89			0.0	0.0	71.42	2.07
ala-1175	1175	54.88	2.83	-1.72	0.0	0.0	62.48	1.91
ala-1205	1205	54.87	2.63	-1.61	0.0	0.0	58.20	2.94
ala-1235	1235	54.86	2.48	-1.79	3.6	0.0	47.81	2.70
ala-1265	1265	54.84	2.45	-1.77	0.0	0.0	57.77	1.66
ala-1295	1295	54.83	2.64	-1.72	4.6	0.0	70.21	2.08
ala-1296	1296	54.83					80.00	2.30
ala-1300	1300	54.83					73.96	1.77
ala-1305	1305	54.83					73.45	3.91
ala-1310	1310	54.83	2.45	-1.63	0.0	0.0	64.78	1.96
ala-1315	1315	54.82	2.45	-1.60			74.12	2.59
ala-1320	1320	54.82					76.88	4.49
ala-1325	1325	54.82	2.49	-1.75			80.17	2.34
ala-1330	1330	54.82	2.24	-1.64	0.0	0.0	68.71	2.65
ala-1335	1335	54.81	2.28	-1.67				
ala-1345	1345	54.81	2.20	-1.67				
ala-1350	1350	54.81	2.13	-1.68	0.0	0.0		
ala-1360	1360	54.80	1.89	-1.68			1.80	12.18
ala-1370	1370	54.80	33.2	-1.2			21.26	10.67
ala-1371	1371	54.80	1.42	-1.50				
ala-1380	1380	54.80	1.40	-1.70			26.14	11.43
ala-1385	1385	54.79	1.18	-2.17				
ala-1390	1390	54.79	0.98	-1.71	7.3	22.5	37.16	8.92
ala-1395	1395	54.79	1.10	-1.94			33.65	9.64
ala-1400	1400	54.79					40.28	8.78
ala-1410	1410	54.78	0.85	-1.72			56.51	7.30
ala-1420	1420	54.78					59.63	7.44

Continued

$\delta^{13}\text{C}$ PALAEOCENE–EOCENE EXCURSIONAppendix. Data table for Figure 1, *continued*

Sample	cm	Age (Myr)	$\delta^{13}\text{C}$	$\delta^{18}\text{O}$	Turnover Rate (%)	(%) Comp. Acarininids	Calcite	Detritus
ala-14425	1425	54.78	0.93	-1.63	9.2	22.5	56.14	8.13
ala-1430	1430	54.78					63.27	8.29
ala-1440	1440	54.77					69.52	5.33
ala-1450	1450	54.77	0.74	-1.70	0.0	32.7	43.12	8.84
ala-1460	1460	54.76					70.28	5.93
ala-1470	1470	54.76					45.80	8.54
ala-1480	1480	54.75	0.97	-1.87	4.6	5.9	42.03	8.93
ala-1490	1490	54.75	0.94	-1.90	30.3	3.3	37.96	9.14
ala-1500	1500	54.73					83.28	3.12
ala-1505	1505	54.73	1.23	-1.76	4.6	0.0	79.46	2.70
ala-1535	1535	54.68	1.61	-1.68	0.0	0.0	74.88	3.64
ala-1570	1570	54.63	1.68	-1.86	0.0	0.0	81.21	3.25
ala-1605	1605	54.58	2.11	-1.63	0.0	0.0	80.47	2.65
ala-1640	1640	54.53	2.13	-1.61	0.0	0.0	81.95	2.93
ala-1665	1665	54.50	2.21	-1.62	4.1	0.0	74.89	4.05
ala-1690	1690	54.46	2.18	-1.55	0.0	0.0	76.85	1.95
ala-1725	1725	54.41	1.99	-1.48	0.0	0.0	76.75	2.53
ala-1750	1750	54.38	2.01	-1.47	3.2	0.0	76.38	1.95
ala-1790	1790	54.32	2.14	-1.52	0.0	0.0	80.09	2.64
ala-1815	1815	54.28	2.16	-1.59	3.0	0.0	80.45	3.12
ala-1860	1860	54.22	1.98	-1.57	2.8	0.0	82.44	3.05
ala-1890	1890	54.18	2.11	-1.52	0.0	0.0	60.22	1.70
ala-1925	1925	54.13	2.34	-1.94	0.0	0.0	80.05	1.64
ala-1955	1955	54.08	1.95	-1.69	0.0	0.0	67.07	5.11
ala-1990	1990	54.03	2.00	-1.56	0.0	0.0	76.99	2.63
ala-2025	2025	53.98	2.15	-1.55	3.0	0.0	81.86	3.32
ala-2060	2060	53.93	1.93	-1.64	0.0	0.0	86.67	2.69
ala-2095	2095	53.88	1.86	-1.62	0.0	0.0	85.66	3.04
ala-2130	2130	53.83	1.99	-1.61	0.0	0.0	85.60	2.53
ala-2165	2165	53.78	1.80	-1.61	3.3	0.0	80.36	1.75
ala-2195	2195	53.74	1.88	-1.70	3.4	0.0	81.06	2.70
ala-2230	2230	53.69	1.88	-1.62	0.0	0.0	84.04	1.83
ala-2260	2260	53.65	1.80	-1.53	0.0	0.0	76.98	2.49
ala-2295	2295	53.60	1.90	-1.39	0.0	0.0	80.52	2.18
ala-2330	2330	53.55	1.92	-1.75	3.4	0.0	83.74	2.84
ala-2360	2360	53.51	1.84	-1.61	0.0	0.0	84.34	2.17
ala-2385	2385	53.47	1.83	-1.61	0.0	0.0	83.41	2.65
ala-2420	2420	53.42	1.69	-1.47	0.0	0.0	88.60	2.09
ala-2450	2450	53.38	1.78	-1.70	2.7	0.0	76.31	3.09
ala-2500	2500	53.31	1.92	-1.64	0.0	0.0	73.40	3.11
ala-2560	2560	53.22	1.74	-1.62	0.0	0.0	88.18	2.98
ala-2620	2620	53.13	1.55	-1.50	0.0	0.0	87.20	2.24
ala-2680	2680	53.05	1.64	-1.53	0.0	0.0	77.50	3.31
ala-2740	2740	52.96	1.33	-1.75	0.0	0.0	27.20	9.77
ala-2800	2800	52.88	1.47	-1.44	1.9	0.0	82.71	1.99
ala-2850	2850	52.81	1.27	-1.73	0.0	0.0	56.45	5.73